CHEMISTRY OF MATERIALS

Article

pubs.acs.org/cm

Hybrid Polyhedral Oligomeric Silsesquioxanes–Imides with Tailored Intercage Spacing for Sieving of Hot Gases

Michiel J. T. Raaijmakers,[†] Matthias Wessling,[‡] Arian Nijmeijer,[†] and Nieck E. Benes*,[†]

[†]Inorganic Membranes, Department of Science and Technology, MESA+ Institute for Nanotechnology,University of Twente, P.O. Box 217, 7500 AE Enschede, The Netherlands

[‡]DWI – Leibniz-Institute for Interactive Materials, Forckenbeckstrasse 50, 52074 Aachen, Germany

Supporting Information

ABSTRACT: Macromolecular network rigidity of synthetic membranes is essential for sieving of hot gases. Hyper-cross-linked polyPOSS–imide membranes with tailored intercage spacing are presented. The length and flexibility of their imide bridges enables tuning of gas permeability and selectivity in a broad temperature range. The facile synthesis allows for large-scale production of membranes designed for specific process conditions.

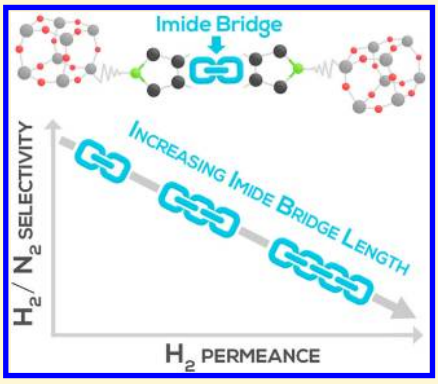

INTRODUCTION

Sieving of hot gases requires membranes with moderated macromolecular dynamics at elevated temperatures.[1] Recently, we have presented ultrathin polyPOSS–imide hybrid membranes that allow gas separation in a broad temperature range.[2] The polyPOSS–imide membranes consist of a giant molecular network of polyhedral oligomeric silsesquioxanes (POSS), covalently linked by imide bridges. The hyper-cross-linked network characteristics allow persistence of gas separation performance up to 300 °C. At such temperatures size-sieving selectivity of organic polymeric membranes disappears, due to the loss in their chain rigidity.[3] Here, we demonstrate that we can tailor the gas sieving performance of nanoscale hybrid membranes via selection of the imide bridge that connects the POSS cages. The length and flexibility of the imide bridges directly affect the macromolecular dynamics and intercage distance of the giant network. In turn, this enables tuning of gas permeability and selectivity in a broad temperature range. The facile nature of the technique used for membrane synthesis allows for large-scale and defect-free membrane production, with properties tailored to fit the process requirements.

Hybrid materials allow integration of the superior thermomechanical properties of inorganic materials and versatile organic polymer segments. The physical dispersion of inorganic nanoparticles in polymers allows for materials synthesis with properties that are a combination of the individual components.[4] Superior properties can be obtained by incorporation of nanoscale inorganic moieties as an intrinsic part of the polymeric network.[5] The octahedral symmetry of polyhedral oligomeric silsesquioxanes (POSS) and the wide array of functional groups they are decorated with permit covalent bond formation in three dimensions. Here, we use a facile interfacial polymerization reaction that allows for production of nanoscale-hybrid ultrathin films.[2,6] The hybrid membranes are prepared by interfacial polycondensation of octa-ammonium POSS in water and a dianhydride in toluene, resulting in the formation of a polyPOSS–(amic acid) membrane film. The high reactivity of the monomers allows for rapid formation of inherently defect-free membranes. Inhibition of reactant diffusion upon film formation impedes further film growth, limiting the film thickness to several hundred nanometers.

EXPERIMENTAL SECTION

Synthesis of polyPOSS–Imides by Interfacial Polymerization. Toluene (anhydrous 99.8 wt %, Sigma-Aldrich), pyromellitic dianhydride (PMDA, Sigma-Aldrich), 3,3′,4,4′-biphenyl tetracarboxylic dianhydride (BPDA, Sigma-Aldrich), 4,4′-oxidiphthalic anhydride (ODPA, Sigma-Aldrich), 4,4′-(4,4′-isopropylidenediphenoxy)bis-(phthalic anhydride) (BPADA), 4,4-(hexafluoroisopropylidene) diphthalic anhydride (6-FDA, Sigma-Aldrich), ammonium chloride salt functionalized POSS (OctaAmmonium POSS, Hybrid Plastics (U.S.A.)), and sodium hydroxide (Sigma-Aldrich) were used as received. Free-standing films were prepared using ammonium chloride salt functionalized POSS, which is readily soluble in water. The pH of an aqueous solution of 0.9 wt % ammonium chloride salt functionalized POSS was adjusted using sodium hydroxide (0.1 mol L^{-1}) and subsequently contacted with the dianhydride solution in toluene (0.075 wt %). Supported membranes were produced on

Received: February 26, 2014
Revised: May 20, 2014
Published: May 21, 2014

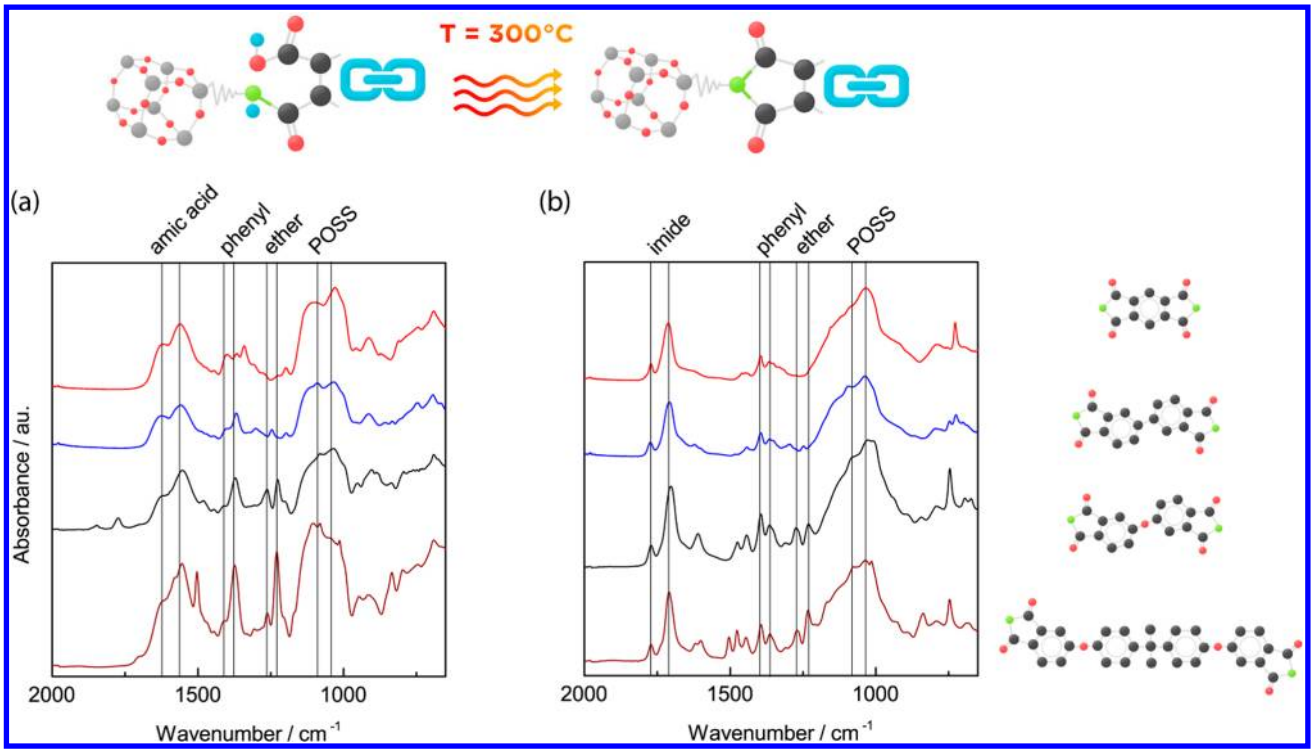

Figure 1. ATR-FTIR absorbance spectra of (a) polyPOSS−(amic)acid and (b) polyPOSS−imide (after 300 °C heat treatment) prepared using PMDA (—), BPDA (—), ODPA (—), and BPADA (—). The bands at 1620 and 1570 cm^{-1} are assigned to N−H bending (1) and C═O stretching (2) of the amide group. After heat treatment the bands at 1620 and 1570 cm^{-1} are substituted by the bands at 1720 and 1780 cm^{-1}, assigned to C═O asymmetric (3) and symmetric (4) stretching of the imide group, respectively. The sharp bands at 1125 and 1040 cm^{-1} can be attributed to the Si−O−Si asymmetric stretching vibrations of polyhedral and ladder silsesquioxane structures, respectively. Partial cleavage of the POSS cages occurs due to hydrolysis by hydroxyl ions.

ceramic membranes (α-alumina discs with a 3-μm-thick γ-alumina layer) by prewetting the porous ceramic material under 0.5 bar vacuum in the aqueous POSS solution for 15 min, followed by contacting with the dianhydride solution in toluene for 5 min. The pore size of the γ-alumina is on the order of several nanometers and allows for defect-free interfacial polymerization membrane formation. The high hydrophilicity of the γ-alumina allows for facile wetting of the pores with the aqueous phase. Thermal conversion of the polyPOSS−(amic acid) to polyPOSS−imide was performed for 2 h at 300 °C under an air atmosphere, at a heating rate of 5 °C min^{-1}.

Materials Characterization. Membrane single gas permeation experiments were performed in a dead-end mode at a trans-membrane pressure of 2 bar and atmospheric pressure at the permeate side. Once the helium permeance remained constant, the other gases (N_2, CH_4, H_2, and CO_2, consecutively) were measured at temperatures between 50 and 300 °C.

■ RESULTS AND DISCUSSION

After film formation by interfacial polymerization, the polyPOSS−(amic acid) is converted to a polyPOSS−imide by thermal treatment at 300 °C. Figure 1 shows the attenuated total reflection−Fourier transform infrared spectroscopy (ATR-FTIR) spectra of the polyPOSS−(amic acid) and polyPOSS−imide materials. The polyPOSS−(amic acid) spectra in Figure 1a show common peaks at identical wave numbers that can be attributed to the POSS cages, the amic acid groups, and the phenyl groups. The differences between the polyPOSS−(amic acid) spectra originate from the different functional groups of the dianhydrides; PMDA contains a 1,2,4,5-substituted phenyl, ODPA contains an ether, and BPADA has quaternary carbon and ether bonds (the complete peak analysis can be found in the Supporting Information). After thermal treatment two distinct imide bands emerge at 1720 and 1780 cm^{-1}. These peaks are attributed to the polyimide carbonyl symmetric and asymmetric stretching, respectively. The vanishing of the amic acid bands at 1620 and 1570 cm^{-1} indicates that complete conversion of the amic acid to imide groups is achieved.[7] Also, the polyPOSS−imide spectra lack carboxylic acid and dianhydride bands, implying that no detectable unreacted dianhydride moieties remain after imidization. The ratios between the POSS and imide peak intensities are similar for all polyPOSS−imides, implying that the number of imide groups on each POSS cage is not strongly affected by differences in reactivity and solubility of the dianhydrides.

The similar degree of POSS interconnectivity is confirmed by X-ray photoelectron spectroscopy (XPS) measurements of ceramic supported polyPOSS−imide membranes (Supporting Information). Deconvoluted nitrogen elemental spectra reveal that, on average, four out of eight functional groups on each POSS cage are converted to imides. The remaining unreacted functional groups are mostly primary amines, of which a slight fraction is protonated. The nitrogen, silica, and carbon elemental compositions derived from the XPS measurement suggest a similar number of imide bridges per POSS molecule, assuming that no unreacted dianhydride groups remain. Both the infrared and XPS spectra reveal that partial hydrolysis of the POSS cage occurs. The wide range of dianhydrides suitable for the interfacial polycondensation of octa-ammonium POSS allows for production of gas separation membranes with a tailored intercage spacing. Figure 2 demonstrates the adaptability of the single gas permeance and selectivity over a broad temperature range, by the use of different imide bridges. Figure 2a shows the gas sieving abilities of the membranes. The

dx.doi.org/10.1021/cm500691e | Chem. Mater. 2014, 26, 3660−3664

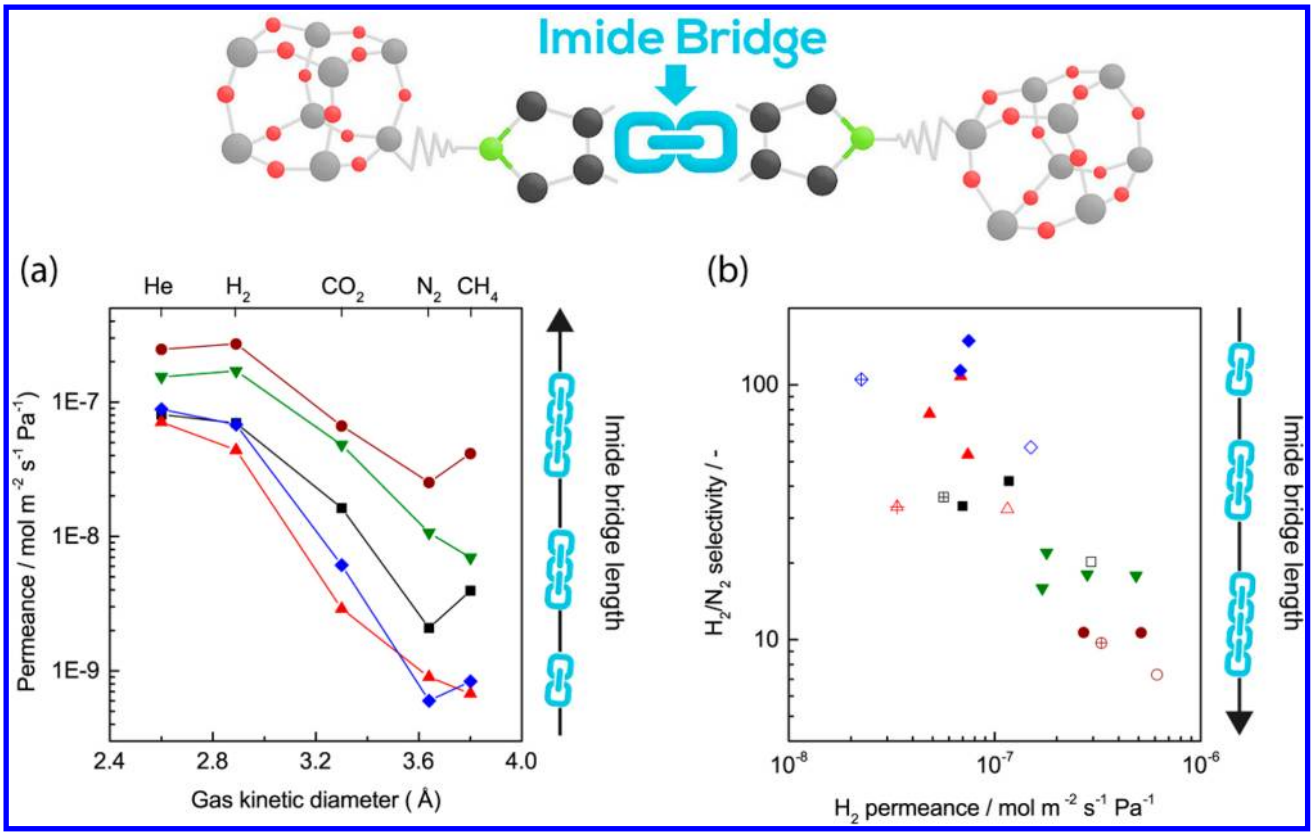

Figure 2. (a) Single gas permeance at 200 °C as a function of gas kinetic diameter for the polyPOSS−imides derived from PMDA (▲), BPDA (◆), ODPA (■), 6FDA (▼), and BPADA (●). All polyPOSS−imides are selective toward smaller kinetic diameter gases. The gas permeance of all gases increases with increasing dianhydride molecular length, supporting the hypothesis that the inter-POSS spacing is a key parameter for the membrane characteristics. (b) The H_2/N_2 ideal gas selectivity as a function of hydrogen permeance at 100 °C (open, crossed symbols), 200 °C (closed symbols), and 300 °C (open symbols) for the polyPOSS−imides derived from the different dianhydrides. The H_2/N_2 selectivity increases with decreasing imide bridge length, while H_2 permeance is lower for the short imide bridges.

gas permeance follows a monotonic decrease with increasing kinetic diameter of the molecules, indicating that molecular separation occurs on the basis of size exclusion. The diffusivity-controlled selectivity was also observed for the 6-FDA based polyPOSS−imides and originates from the hyper-cross-linked network characteristics. The permeance of each gas increases with increasing length of the imide bridges. This indicates that the larger spacing between the POSS cages results in increased permeation. The observation that transport occurs via the organic bridges of the hybrid material is supported by molecular dynamics simulations of gas transport in amino functionalized POSS.[8] Figure 2b shows that the intercage distance also affects the permselectivity. The H_2/N_2 selectivity as a function of the H_2 permeance shows the typical trade-off for molecular sieving membranes. A decrease in permeance, with decreasing length of the imide bridge, concurs with a substantial increase in the H_2/N_2 selectivity. At 100, 200, and 300 °C a similar trade-off between selectivity and permeance can be observed.

The gas permeation data as a function of temperature demonstrates the hyper-cross-linked characteristics of the polyPOSS−imides. Figure 3 shows the Arrhenius plots for the membranes prepared with BPDA and BPADA. The Arrhenius plots for the membranes prepared with PMDA and ODPA are given in the Supporting Information. All membranes showed persistent gas selectivity in the temperature range of 50−300 °C. Thermogravimetric analysis (TGA, Supporting Information) confirms that no material degradation occurs below 300 °C for all polyPOSS−imides. For all membranes the permeances increase with temperature, and an Arrhenius-type temperature dependence is observed for most gases. The membranes based on the shortest linkers, BPDA (Figure 3a) and PMDA (Supporting Information, Figure S1), show similar apparent activation energies for all gases. The absence of any significant changes in the activation energy demonstrates the resilience of these membranes with respect to the operating temperature. This translates into the unsurpassed permselectivities that these membranes display at temperatures up to 300 °C. Figure 3b shows the corresponding permselectivities of H_2/N_2, H_2/CH_4, H_2/CO_2, and CO_2/CH_4 as a function of temperature. Single gas H_2/N_2 and H_2/CH_4 selectivities between 40 and 190 are observed for BPDA and 10−55 for PMDA based membranes, respectively. Most noteworthy, the H_2/N_2 and H_2/CH_4 selectivity predominantly increases with temperature. The H_2/CO_2 selectivities are above 10 over the complete temperature range of 50−300 °C for the BPDA based polyPOSS−imides. Relatively few membrane materials have been characterized in a similar temperature range, due to the limited membrane performance stability at elevated temperatures. In the past few years, data have become available on polybenzimidazole membranes. These membranes exhibit slightly higher selectivities but significantly lower permeances. Also, interesting work has been performed on elevated temperature gas separation with polyimides and polyaramides.[3,9] The performance of these materials is comparable to our hybrid materials but does not persist up to 200 °C.[10]

dx.doi.org/10.1021/cm500691e | *Chem. Mater.* 2014, 26, 3660−3664

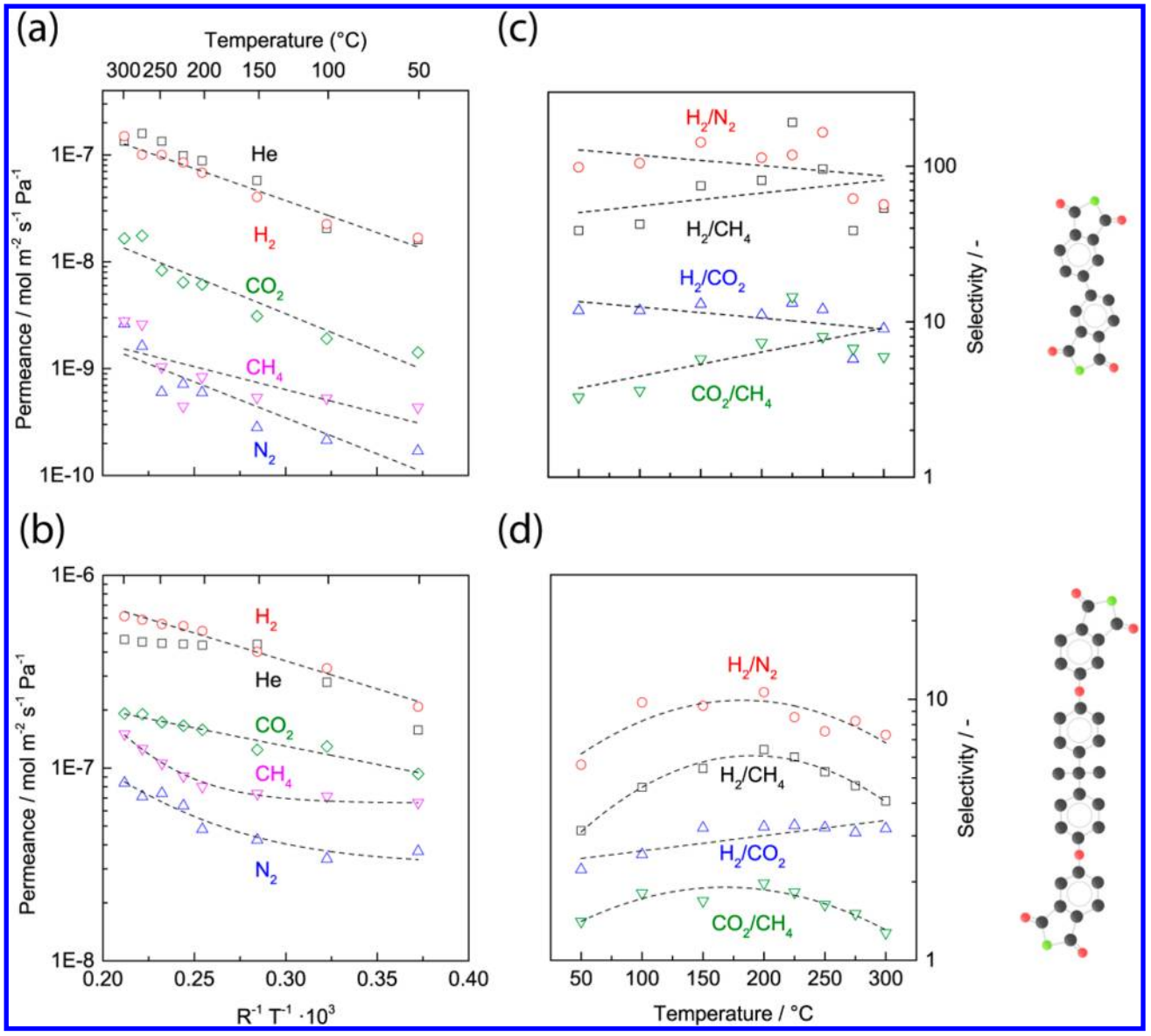

Figure 3. Arrhenius plot of the logarithm of the single gas permeance of He, H_2, CO_2, N_2, and CH_4, as a function of 1000 $R^{-1}T^{-1}$ for the polyPOSS−imides derived from BPDA (a), and BPADA (b). The apparent activation energies for gas permeance are given in Table S1 in the Supporting Information, calculated from the slope of ln(permeance) as a function of $R^{-1}T^{-1}$. The corresponding ideal gas selectivities of H_2/N_2, H_2/CH_4, H_2/CO_2, and CO_2/CH_4 as a function of temperature for the polyPOSS−imides derived from BPDA (c) and BPADA (d). The dashed lines are drawn as a guide to the eye.

There is a range of rigid polymers, such as poly(benzoxazole)s and poly(benzoxazole-*co*-imides), that have potential for high temperature gas separation.[11] Yet, currently there is a lack of performance data at high temperatures.

The polyPOSS−imides allow for facile tailoring of the rigidity and spacing of the segments that connect the POSS cages. The short imide bridges constrain macromolecular motions that would allow for permeation of larger kinetic diameter gas molecules. This is in contrast to longer imide bridges, ODPA and BPADA. These longer bridges display temperature dependent apparent activation energies for the gas permeance of the larger molecules, N_2 and CH_4. At elevated temperature the molecular mobility of the longer bridges is more affected by an increase in temperature, as compared to the mobility of the short imide bridges. This in line with the variation in the coherence length found for conventional polyimides, obeying the order PMDA > BPDA > ODPA > BPADA.[12] The augmented network mobility is manifested by a contribution to the apparent energy of activation, reflected by an increased permeation. This effect is most pronounced for the larger molecules that suffer the most from size exclusion. At lower temperatures the molecular motions of the network are less pronounced, and their contribution to the apparent energy of activation diminishes. This is reflected by lower apparent energies of activation of N_2 and CH_4 permeance at temperatures below 150 °C. Differential scanning calorimetry (DSC) measurements on all polyPOSS−imides (Supporting Information) do not show any sharp transitions, indicating the network dynamics only change gradually. The absence of a glass transition at temperatures up to 300 °C can therefore not be the origin of the change in an apparent activation energy. The transition in activation energies results in a maximum selectivity of H_2/N_2 and H_2/CH_4 of ODPA and BPADA (d) based polyPOSS−imides at a temperature around 150 °C. The

dx.doi.org/10.1021/cm500691e | *Chem. Mater.* 2014, 26, 3660−3664

different selectivities of the polyPOSS−imides as a function of temperature stresses the importance of the network dynamics for membrane performance, even in a system with relatively short flexible moieties. This understanding is essential for selecting the suitable imide bridge and allows for a broad range of applications and operating conditions.

In conclusion, the polyPOSS−imide membranes allow unprecedented gas sieving performance at elevated temperatures. Their facile synthesis allows for large-scale production of membranes designed for specific process conditions. The molecular sieving characteristics can be tailored by varying the intercage spacing, via the length of the imide bridge. The persistence of gas separation stability up to 300 °C underlines the hyper-cross-linked periodic network characteristics of the covalently bound rigid POSS. The simple and reliable synthesis method potentially allows for large-scale production of a new generation of tailor-made hybrid membranes for industrial scale applications that require sieving of hot gases.

■ ASSOCIATED CONTENT

Supporting Information

Material analysis using single gas permeation analysis, differential scanning calorimetry, thermal gravimetric analysis, X-ray photoelectron spectroscopy, and full infrared peak analysis. This material is available free of charge via the Internet at http://pubs.acs.org

■ AUTHOR INFORMATION

Corresponding Author

*E-mail: n.e.benes@utwente.nl.

Notes

The authors declare no competing financial interest.

■ ACKNOWLEDGMENTS

This research has received funding from the European Union Seventh Framework Programme FP7-NMP-2010-Large-4 under Grant Agreement no. 263007 (acronym CARENA). M.W. acknowledges support through the Alexander von Humboldt Foundation.

■ REFERENCES

(1) Maier, G. *Angew. Chem., Int. Ed.* **1998**, *37* (21), 2961−2974.

(2) Raaijmakers, M. J. T.; Hempenius, M. A.; Schön, P. M.; Vancso, G. J.; Nijmeijer, A.; Wessling, M.; Benes, N. E. *J. Am. Chem. Soc.* **2013**, *136* (1), 330−335.

(3) Koros, W. J.; Woods, D. G. *J. Membr. Sci.* **2001**, *181* (2), 157−166.

(4) (a) Le, N. L.; Chung, T. S. *J. Membr. Sci.* **2014**, *454*, 62−73. (b) Lee, Y. J.; Huang, J. M.; Kuo, S. W.; Chang, F. C. *Polymer* **2005**, *46* (23), 10056−10065. (c) Chua, M. L.; Shao, L.; Low, B. T.; Xiao, Y.; Chung, T. S. *J. Membr. Sci.* **2011**, *385−386* (1), 40−48. (d) Li, Y.; Chung, T. S. *Int. J. Hydrogen Energy* **2010**, *35* (19), 10560−10568.

(5) (a) Laine, R. M.; Roll, M. F. *Macromolecules* **2011**, *44* (5), 1073−1109. (b) Nischang, I.; Brüggemann, O.; Teasdale, I. *Angew. Chem., Int. Ed.* **2011**, *50* (20), 4593−4596. (c) Oaten, M.; Choudhury, N. R. *Macromolecules* **2005**, *38* (15), 6392−6401. (d) Wu, G.; Su, Z. *Chem. Mater.* **2006**, *18* (16), 3726−3732. (e) Zhang, C.; Babonneau, F.; Bonhomme, C.; Laine, R. M.; Soles, C. L.; Hristov, H. A.; Yee, A. F. *J. Am. Chem. Soc.* **1998**, *120* (33), 8380−8391.

(6) Dalwani, M.; Zheng, J.; Hempenius, M.; Raaijmakers, M. J. T.; Doherty, C. M.; Hill, A. J.; Wessling, M.; Benes, N. E. *J. Mater. Chem.* **2012**, *22* (30), 14835−14838.

(7) Diaham, S.; Locatelli, M. L.; Lebey, T.; Malec, D. *Thin Solid Films* **2011**, *519* (6), 1851−1856.

(8) Neyertz, S.; Gopalan, P.; Brachet, P.; Kristiansen, A.; Männle, F.; Brown, D. *Soft Mater.* **2014**, *12* (1), 113−123.

(9) Rezac, M. E.; Koros, W. J.; Miller, S. J. *J. Membr. Sci.* **1994**, *93* (2), 193−201.

(10) (a) Berchtold, K. A.; Singh, R. P.; Young, J. S.; Dudeck, K. W. *J. Membr. Sci.* **2012**, *415−416*, 265−270. (b) Kumbharkar, S. C.; Liu, Y.; Li, K. *J. Membr. Sci.* **2011**, *375* (1−2), 231−240. (c) Li, X.; Singh, R. P.; Dudeck, K. W.; Berchtold, K. A.; Benicewicz, B. C. *J. Membr. Sci.* **2014**, *461*, 59−68.

(11) (a) Calle, M.; Doherty, C. M.; Hill, A. J.; Lee, Y. M. *Macromolecules* **2013**, *46* (20), 8179−8189. (b) Calle, M.; Lozano, A. E.; Lee, Y. M. *Eur. Polym. J.* **2012**, *48* (7), 1313−1322. (c) Joseph, W. D.; Abed, J. C.; Mercier, R.; McGrath, J. E. *Polymer* **1994**, *35* (23), 5046−5050. (d) Kim, S.; Han, S. H.; Lee, Y. M. *J. Membr. Sci.* **2012**, *403−404*, 169−178.

(12) Ree, M.; Kim, K.; Woo, S. H.; Chang, H. *J. Appl. Phys.* **1997**, *81* (2), 698−708.